Assessment of corneal dynamics with high-speed swept source Optical Coherence Tomography combined with an air puff system

David Alonso-Caneiro,[1,2] Karol Karnowski,[1] Bartlomiej J. Kaluzny,[3] Andrzej Kowalczyk,[1] and Maciej Wojtkowski[1,*]

[1]*Institute of Physics, Nicolaus Copernicus University, ul. Grudziadzka 5/7, PL-87-100 Torun, Poland*
[2]*Contact Lens and Visual Optics Laboratory, School of Optometry, Queensland University of Technology, Brisbane, Australia*
[3]*Department of Ophthalmology, Collegium Medicum, Nicolaus Copernicus University, Bydgoszcz, Poland*
[*]*maciej.wojtkowski@fizyka.umk.pl*

Abstract: We present a novel method and instrument for *in vivo* imaging and measurement of the human corneal dynamics during an air puff. The instrument is based on high-speed swept source optical coherence tomography (ssOCT) combined with a custom adapted air puff chamber from a non-contact tonometer, which uses an air stream to deform the cornea in a non-invasive manner. During the short period of time that the deformation takes place, the ssOCT acquires multiple A-scans in time (M-scan) at the center of the air puff, allowing observation of the dynamics of the anterior and posterior corneal surfaces as well as the anterior lens surface. The dynamics of the measurement are driven by the biomechanical properties of the human eye as well as its intraocular pressure. Thus, the analysis of the M-scan may provide useful information about the biomechanical behavior of the anterior segment during the applanation caused by the air puff. An initial set of controlled clinical experiments are shown to comprehend the performance of the instrument and its potential applicability to further understand the eye biomechanics and intraocular pressure measurements. Limitations and possibilities of the new apparatus are discussed.

OCIS codes: (170.4500) Optical coherence tomography; (170.3880) Medical and biological imaging; (170.4470) Ophthalmology.

References and links

1. D. A. Luce, "Determining in vivo biomechanical properties of the cornea with an ocular response analyzer," J. Cataract Refract. Surg. **31**(1), 156–162 (2005).
2. R. L. Stamper, "A history of intraocular pressure and its measurement," Optom. Vis. Sci. **88**(1), E16–E28 (2011).
3. D. Ortiz, D. Pinero, M. H. Shabayek, F. Arnalich-Montiel, and J. L. Alió, "Corneal biomechanical properties in normal, post-laser in situ keratomileusis, and keratoconic eyes," J. Cataract Refract. Surg. **33**(8), 1371–1375 (2007).
4. K. F. Damji, R. H. Muni, and R. M. Munger, "Influence of corneal variables on accuracy of intraocular pressure measurement," J. Glaucoma **12**(1), 69–80 (2003).
5. G. J. Orssengo and D. C. Pye, "Determination of the true intraocular pressure and modulus of elasticity of the human cornea in vivo," Bull. Math. Biol. **61**(3), 551–572 (1999).
6. J. Liu and C. J. Roberts, "Influence of corneal biomechanical properties on intraocular pressure measurement: quantitative analysis," J. Cataract Refract. Surg. **31**(1), 146–155 (2005).
7. F. A. La Rosa, R. L. Gross, and S. Orengo-Nania, "Central corneal thickness of Caucasians and African Americans in glaucomatous and nonglaucomatous populations," Arch," Ophthalmol-chic **119**, 23–27 (2001).
8. M. M. Whitacre, R. A. Stein, and K. Hassanein, "The effect of corneal thickness on applanation tonometry," Am. J. Ophthalmol. **115**(5), 592–596 (1993).
9. F. A. Medeiros and R. N. Weinreb, "Evaluation of the influence of corneal biomechanical properties on intraocular pressure measurements using the ocular response analyzer," J. Glaucoma **15**(5), 364–370 (2006).

#146816 - $15.00 USD Received 29 Apr 2011; revised 26 Jun 2011; accepted 27 Jun 2011; published 11 Jul 2011

10. M. R. Ford, W. J. Dupps, Jr., A. M. Rollins, A. S. Roy, and Z. Hu, "Method for optical coherence elastography of the cornea," J. Biomed. Opt. **16**(1), 016005–016007 (2011).
11. X. He and J. Liu, "A quantitative ultrasonic spectroscopy method for noninvasive determination of corneal biomechanical properties," Invest. Ophthalmol. Vis. Sci. **50**(11), 5148–5154 (2009).
12. K. W. Hollman, S. Y. Emelianov, J. H. Neiss, G. Jotyan, G. J. R. Spooner, T. Juhasz, R. M. Kurtz, and M. O'Donnell, "Strain imaging of corneal tissue with an ultrasound elasticity microscope," Cornea **21**(1), 68–73 (2002).
13. R. Ambrósio, Jr., L. P. Nogueira, D. L. Caldas, B. M. Fontes, A. Luz, J. O. Cazal, M. R. Alves, and M. W. Belin, "Evaluation of corneal shape and biomechanics before LASIK," Int. Ophthalmol. Clin. **51**(2), 11–38 (2011).
14. C. J. Roberts, A. M. Mahmoud, I. Ramos, D. Caldas, R. Siqueira da Silva, and J. R. Ambrósio, "Factors influencing corneal deformation and estimation of intraocular pressure," in *ARVO*(2011), pp. e-abstract 4384.
15. I. Grulkowski, M. Gora, M. Szkulmowski, I. Gorczynska, D. Szlag, S. Marcos, A. Kowalczyk, and M. Wojtkowski, "Anterior segment imaging with Spectral OCT system using a high-speed CMOS camera," Opt. Express **17**(6), 4842–4858 (2009).
16. P. Targowski, M. Wojtkowski, A. Kowalczyk, T. Bajraszewski, M. Szkulmowski, and I. Gorczynska, "Complex spectral OCT in human eye imaging in vivo," Opt. Commun. **229**(1-6), 79–84 (2004).
17. J. A. Izatt, M. R. Hee, E. A. Swanson, C. P. Lin, D. Huang, J. S. Schuman, C. A. Puliafito, and J. G. Fujimoto, "Micrometer-scale resolution imaging of the anterior eye in vivo with optical coherence tomography," Arch. Ophthalmol-chic **112**, 1584–1589 (1994).
18. D. Huang, Y. Li, and S. Radhakrishnan, "Optical coherence tomography of the anterior segment of the eye," Ophthalmol. Clin. North Am. **17**(1), 1–6 (2004).
19. M. R. Hee, J. A. Izatt, E. A. Swanson, D. Huang, J. S. Schuman, C. P. Lin, C. A. Puliafito, and J. G. Fujimoto, "Optical coherence tomography of the human retina," Arch. Ophthalmol-chic **113**, 325–332 (1995).
20. J. M. Gonzalez-Meijome, A. Cerviño, G. Carracedo, A. Queiros, S. Garcia-Lázaro, and T. Ferrer-Blasco, "High-resolution spectral domain optical coherence tomography technology for the visualization of contact lens to cornea relationships," Cornea **29**(12), 1359–1367 (2010).
21. B. J. Kaluzny, J. J. Kaluzny, A. Szkulmowska, I. Gorczynska, M. Szkulmowski, T. Bajraszewski, P. Targowski, and A. Kowalczyk, "Spectral optical coherence tomography: a new imaging technique in contact lens practice," Ophthalmic Physiol. Opt. **26**(2), 127–132 (2006).
22. S. Ortiz, D. Siedlecki, I. Grulkowski, L. Remon, D. Pascual, M. Wojtkowski, and S. Marcos, "Optical distortion correction in optical coherence tomography for quantitative ocular anterior segment by three-dimensional imaging," Opt. Express **18**(3), 2782–2796 (2010).
23. A. de Castro, S. Ortiz, E. Gambra, D. Siedlecki, and S. Marcos, "Three-dimensional reconstruction of the crystalline lens gradient index distribution from OCT imaging," Opt. Express **18**(21), 21905–21917 (2010).
24. S. Radhakrishnan, A. M. Rollins, J. E. Roth, S. Yazdanfar, V. Westphal, D. S. Bardenstein, and J. A. Izatt, "Real-time optical coherence tomography of the anterior segment at 1310 nm," Arch. Ophthalmol-chic **119**, 1179–1185 (2001).
25. M. Gora, K. Karnowski, M. Szkulmowski, B. J. Kaluzny, R. Huber, A. Kowalczyk, and M. Wojtkowski, "Ultra high-speed swept source OCT imaging of the anterior segment of human eye at 200 kHz with adjustable imaging range," Opt. Express **17**(17), 14880–14894 (2009).
26. Y. Yasuno, V. D. Madjarova, S. Makita, M. Akiba, A. Morosawa, C. Chong, T. Sakai, K. P. Chan, M. Itoh, and T. Yatagai, "Three-dimensional and high-speed swept-source optical coherence tomography for in vivo investigation of human anterior eye segments," Opt. Express **13**(26), 10652–10664 (2005).
27. C. M. Eigenwillig, W. Wieser, B. R. Biedermann, and R. Huber, "Subharmonic Fourier domain mode locking," Opt. Lett. **34**(6), 725–727 (2009).
28. R. Huber, D. C. Adler, and J. G. Fujimoto, "Buffered Fourier domain mode locking: Unidirectional swept laser sources for optical coherence tomography imaging at 370,000 lines/s," Opt. Lett. **31**(20), 2975–2977 (2006).
29. R. Huber, M. Wojtkowski, and J. G. Fujimoto, "Fourier Domain Mode Locking (FDML): A new laser operating regime and applications for optical coherence tomography," Opt. Express **14**(8), 3225–3237 (2006).
30. R. C. Lin, M. A. Shure, A. M. Rollins, J. A. Izatt, and D. Huang, "Group index of the human cornea at 1.3-microm wavelength obtained in vitro by optical coherence domain reflectometry," Opt. Lett. **29**(1), 83–85 (2004).
31. J. Ø. Hjortdal, "Regional elastic performance of the human cornea," J. Biomech. **29**(7), 931–942 (1996).
32. J. Liu and X. He, "Corneal stiffness affects IOP elevation during rapid volume change in the eye," Invest. Ophthalmol. Vis. Sci. **50**(5), 2224–2229 (2009).
33. A. Faucher, J. Grégoire, and P. Blondeau, "Accuracy of Goldmann tonometry after refractive surgery," J. Cataract Refract. Surg. **23**(6), 832–838 (1997).
34. R. Montés-Micó and W. N. Charman, "Intraocular pressure after excimer laser myopic refractive surgery," Ophthalmic Physiol. Opt. **21**(3), 228–235 (2001).
35. J. B. Randleman, "Post-laser in-situ keratomileusis ectasia: current understanding and future directions," Curr. Opin. Ophthalmol. **17**(4), 406–412 (2006).
36. C. Schweitzer, C. J. Roberts, A. M. Mahmoud, J. Colin, S. Maurice-Tison, and J. Kerautret, "Screening of forme fruste keratoconus with the ocular response analyzer," Invest. Ophthalmol. Vis. Sci. **51**(5), 2403–2410 (2010).

#146816 - $15.00 USD Received 29 Apr 2011; revised 26 Jun 2011; accepted 27 Jun 2011; published 11 Jul 2011

1. Introduction

Accurate value of intraocular pressure (IOP) is a crucial clinical parameter for the screening, diagnosis and management of glaucoma, which is a blinding condition associated with elevated IOP [1, 2]. A range of different tonometers are widely used in clinical ophthalmic practice to measure the IOP [2]. For a comprehensive review on intraocular pressure measurements the reader is referred to a recently published article written by Stamper [2]. One of the commonly used tonometry modalities is non-contact tonometry [2], which uses an air puff to applanate the cornea. Shortly after, the air pump shuts off and the pressure declines in a smooth manner. As the pressure decreases, the cornea returns to its normal state. By means of a light source, the instrument monitors the dynamic behavior of the anterior surface of the cornea and provides an estimate of the IOP. In standard non-contact tonometers, a beam of light is projected onto the corneal apex and its reflectivity is measured by a photodiode. The two points of maximum reflection (during the inward/outward movement) indicate when the cornea is flat (i.e. applanated) and can also be used to calculate parameters which describe corneal biomechanical properties, such as corneal hysteresis [1] and corneal resistance factor [3].

The IOP measurement principle in non-contact tonometry is based on the relation between the applied force (the air-puff) and the response from the eye's internal pressure (IOP). This simplified principle, directly derived from the basic mechanics [4], was the initial fundament of tonometry. Although nowadays, it is well known that the eye's biomechanical properties can influence the IOP recording and should also be taken into consideration [4–6]. For example, the corneal thickness [4, 6–8] and, the radius of curvature of the cornea [9] and the viscoelastic properties of the eye [6, 10–12] play an important role in the dynamics of the anterior segment during tonometry. Additionally to extract information about the IOP, some of current tonometers assume certain anterior segment dimensions and corneal properties, based on population averages. Unfortunately, these assumptions can potentially produce an error on the estimates of IOP [6]. To overcome this error, different IOP indicators have been proposed [1], alternatively the clinician can take extra ocular measurements (i.e. pachymetry, corneal radius of curvature) to manually compensate for deviations [2].

To date none of the commonly used tonometers take simultaneous recordings of corneal layers dynamics. Only recently, a new commercial instrument that combines ultra high-speed Scheimpflug recording to monitor corneal deformation in response to an air pulse has been proposed [13]. Although little information is available about this instrument, it highlights the interest for new technologies to monitor corneal layers during non-contact tonometry. Potentially such apparatus could be used to study the relation between biomechanics of the eye during the IOP measurement [14].

In the recent years optical coherence tomography (OCT) techniques have been developed to image the anterior [15–18] and posterior surface of the eye [19]. OCT is an imaging technique that allows micrometer resolution with millimeter imaging depth, making it a very powerful tool to image both segments of the human eye. This non-invasive optical method, has already been used to image the anterior segment in multiple types of application such as contact lens imaging [20, 21], topography estimation [22], crystalline lens characterization [23], irido-corneal angle and sclera imaging [18, 24]. Swept source OCT (ssOCT), which is a Fourier-domain modality that uses wavelength tunable lasers, has proved its potential use for structural imaging of the anterior segment [15, 25, 26]. Especially a 1310 nm wavelength reduces the amount of signal scattering, allowing better penetration into turbid tissue, such as the iris, sclera and anterior chamber angle [18, 24]. Since high repetition rates of swept sources are feasible (up to several hundreds of kHz for Fourier Domain Mode-Locking lasers) [27–29], ssOCT becomes promising for functional analysis of the anterior segment, especially for rapid dynamic measurements like tonometry recordings that take approximately 20 ms.

#146816 - $15.00 USD Received 29 Apr 2011; revised 26 Jun 2011; accepted 27 Jun 2011; published 11 Jul 2011

This paper reports a novel apparatus that combines ssOCT with an air puff chamber, which was purposely adapted from a non-contact tonometer. The instrument allows imaging of axial scans along the central point of the applied air stream, where the corneal displacement is the most pronounced. A purpose-built prototype ssOCT working at a central wavelength of 1310 nm, combined with the air-puff module, is used to acquire information about the anterior segment dynamics during the measurement. The axial resolution of the system is 9 μm in air with an imaging range of approximately 9 mm. During the 20 ms of applanation time, an M-scan of around 1000 A-scans is recorded. Furthermore, we demonstrate the applicability of such an instrument to evaluate the biomechanics of the human cornea and its prospective use to enhance IOP measurements.

2. Methods

2.1 Experimental setup

Figure 1 shows the experimental setup of the swept source OCT combined with the air puff system. A commercially available short cavity swept source laser at 1300 nm (AXSUN Technologies Inc., Billerica, MA) is used as a light source. The laser operates at 50 kHz with a 100 nm optical bandwidth. It delivers light for the dual interferometric OCT system via an 80/20 fiber coupler. One interferometer is used for anterior segment imaging, while the second is used in common path mode to generate reference fringe pattern on a glass plate surfaces. Before the fast Fourier transfrom is performed, to obtain the structural information, the reference fringes have to be remap to achieve equidistant spacing in the wavenumber space [25].

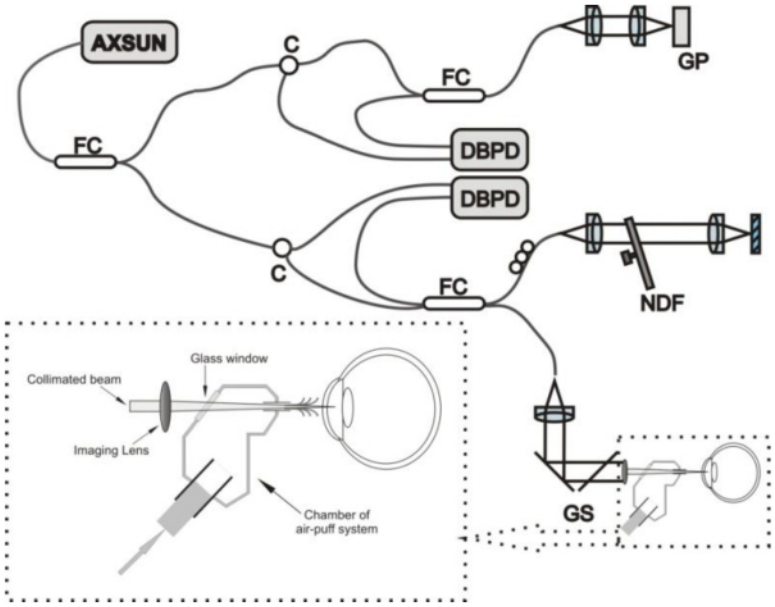

Fig. 1. Schematic diagram of the swept source OCT instrument combined with the air puff system from a commercial tonometer. (AXSUN – commercial swept source laser at 1300nm, FC – Fiber Coupler, C – Circulator, DBPD – Dual-balanced Photo Diode, NDF – Neutral Density Filter, GP – Glass Plate, GS – XY Galvoscanners.)

The sample arm of the first interferometer is merged with the air puff mechanical module extracted from a commercial tonometer (XPert NCT; Reichert Inc., Buffalo, NY). The imaging beam runs through a glass window and exits the chamber through the 3 mm diameter air-pipe that delivers the puff. This approach ensures that the OCT measurement is taken at

#146816 - $15.00 USD Received 29 Apr 2011; revised 26 Jun 2011; accepted 27 Jun 2011; published 11 Jul 2011

the center of applanation. To improve the performance of the system, the original window of the air puff chamber was replaced by a glass transparent to light at 1300 nm.

An electronic circuit that provides a high-voltage pulse to drive the motor for the air puff system was purposely built. The circuit can be controlled externally via a digital input. This input was used to synchronize with the OCT system via the AD converter card that was triggered with the laser frequency. Fringe signals were detected with dual-balance photodiodes (Thorlabs Inc., North Newton, NJ; 75 MHz and 100 MHz) and subsequently acquired and digitized with a dual channel acquisition board (Gage Applied Inc., Lockport, IL; Gage Compuscope 14200, 200 Ms/s, 14 bit resolution).

Sensitivity of the system measured for average 2.5 mW optical power illuminating the sample was measured to be 102 dB at 12 µs exposure time. The axial resolution of the system in air was 9 µm.

2.2 Imaging, alighment setup and surface dynamic segmentation

The applied air stream drives the corneal dynamics. Thus, it is crucial to have a repeatable air pulse applied to the eye each time, especially if the measurements need to be compared. The factors, which determine the air stream characteristics, are related to the instrument's hardware design.

The applanated area is related to the dimension of the pipe and the distance pipe-cornea that was set to remain constant for all the acquired measurements. The applanation pressure, which determines the cornea's displacement, should be similar across measurements. A circuit was designed to trigger the engine with the same high voltage pulse characteristic each time and a reference pipe was connected to the chamber of the air puff to monitor and convert the applied pressure into an electrical signal. To achieve this, the original pressure sensor form the non-contact tonometer was adapted to obtain a reference pressure signal. The circuit provides an analog output that is proportional to the applied pressure. Figure 2(a) presents the mean value and standard deviation of the normalized applied pressure for six consecutive measurements. A reasonably repeatable air stream is observed across six consecutive recordings.

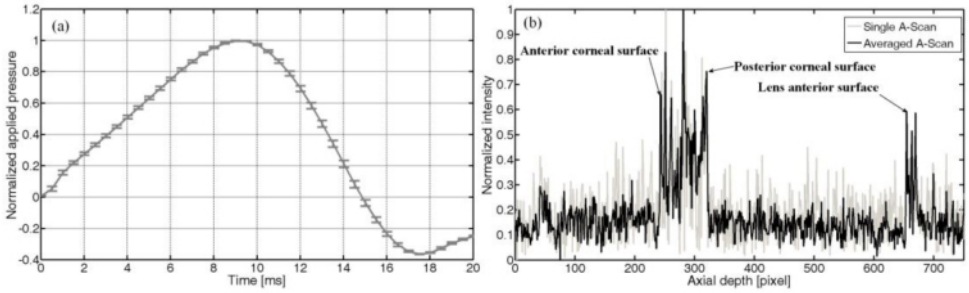

Fig. 2. (a) Time dependent response of the applied pressure in the air puff system measured with the reference pressure sensor. Data were acquired for six consecutive readings of the applied pressure. Vertical bars indicate value of ± 1 Standard Deviation (SD) of the mean, which is plotted as a continuous line. (b) Comparison of a single A-scan and an A-scan averaged with three pre and three post A-scans, to reduce speckle.

The alignment protocol is fundamental to obtain repeatable recordings. The operator follows the following procedure. To allow pupil constriction, the room was kept under photopic conditions. The subject places his/her head on the mechanical headrest (3 axis of movement). Then, the operator aligns the subject's measured eye with the fixation light that runs through the pipe. This first step ensures that the eye's optical axis and the instrument's axis are collinear. Using the preview mode, (pair of horizontal and vertical B-scans crossed in the center) the operator completes the alignment, making sure that the M-scan is taken with a close proximity to the apex of the cornea. Additionally, the operator can adjust the optical

#146816 - $15.00 USD Received 29 Apr 2011; revised 26 Jun 2011; accepted 27 Jun 2011; published 11 Jul 2011

path length difference to ensure that the distance pipe-cornea remains the same for all measurements.

The ssOCT system was set to image the temporal changes of the corneal surfaces and the anterior surface of the crystalline lens at the central point of the applied air stream. Figure 3 shows the recorded M-scan for the anterior segment of the human eye during the measurement. An automatic segmentation procedure was developed to detect the anterior surface position. The procedure works on each of the A-scans detecting the peaks that correspond to each of the surfaces. Before the peak detection, to reduce the speckle noise an average of three pre and three post A-scans that surround the desired A-scan is calculated. Figure 2(b) shows an example of a single A-scan before and after the averaging procedure.

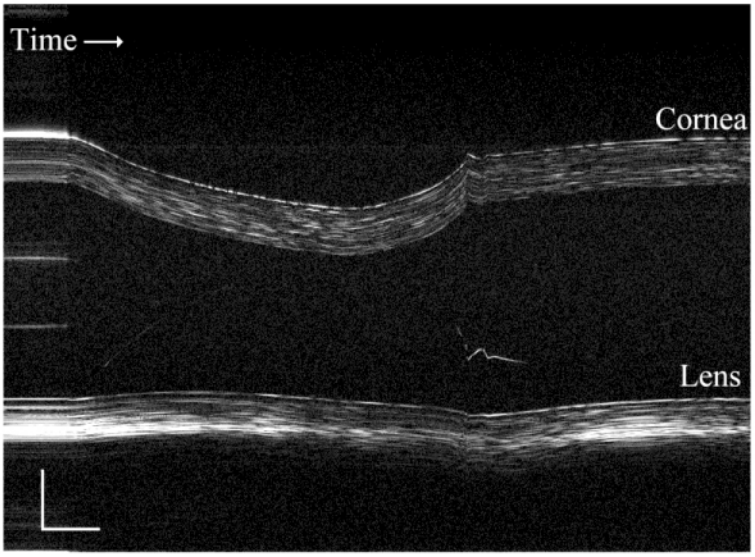

Fig. 3. M-scan (1300 A-scans) recording of the eye's anterior segment, showing the surface motion during the measurement. The scales bars represent 1mm x 2 ms. The M-scan was not corrected from refraction index.

Once the surfaces have been detected, the changes in position (dynamics) of the different surface can be observed. Figure 4 shows the three surface dynamics; anterior corneal surface, posterior corneal surface and anterior surface of the crystalline lens, during the 20 ms interval of the corneal applanation/recovery process. The dynamics of the anterior segment applanation/recovery can be analyzed for each of the segmented surfaces separately. For this image, each of the segmented layers was corrected for refraction errors to obtain the real geometry (i.e. convert pixel to millimeter). Refractive indices of the cornea (n_c=1.389) and aqueous humor (n_{ah}=1.343), which were calculated at 1300 nm [30], were used to recalculate the in-depth axis. The traces are presented as a relative displacement, in which the initial A-scan is used as reference. While correcting for refraction it is assumed that the A-scan was acquired with close proximity to the apex of the cornea (along the optical axis). Thus, we did not account for the incident angle.

#146816 - $15.00 USD Received 29 Apr 2011; revised 26 Jun 2011; accepted 27 Jun 2011; published 11 Jul 2011

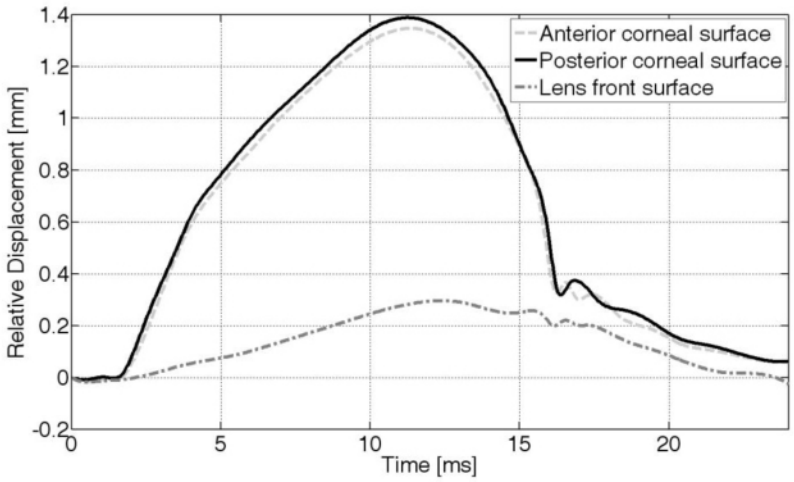

Fig. 4. Relative displacement of the cornea and lens surfaces dynamics during the measurement after correction for refraction.

3. Results

To evaluate the instrument's performance and to understand the nature of the measurement a set of controlled experiments was performed. Subjects were recruited from the students and staff of the university. Approval from the university human research ethics committee was obtained prior to commencement of the study.

#146816 - $15.00 USD Received 29 Apr 2011; revised 26 Jun 2011; accepted 27 Jun 2011; published 11 Jul 2011

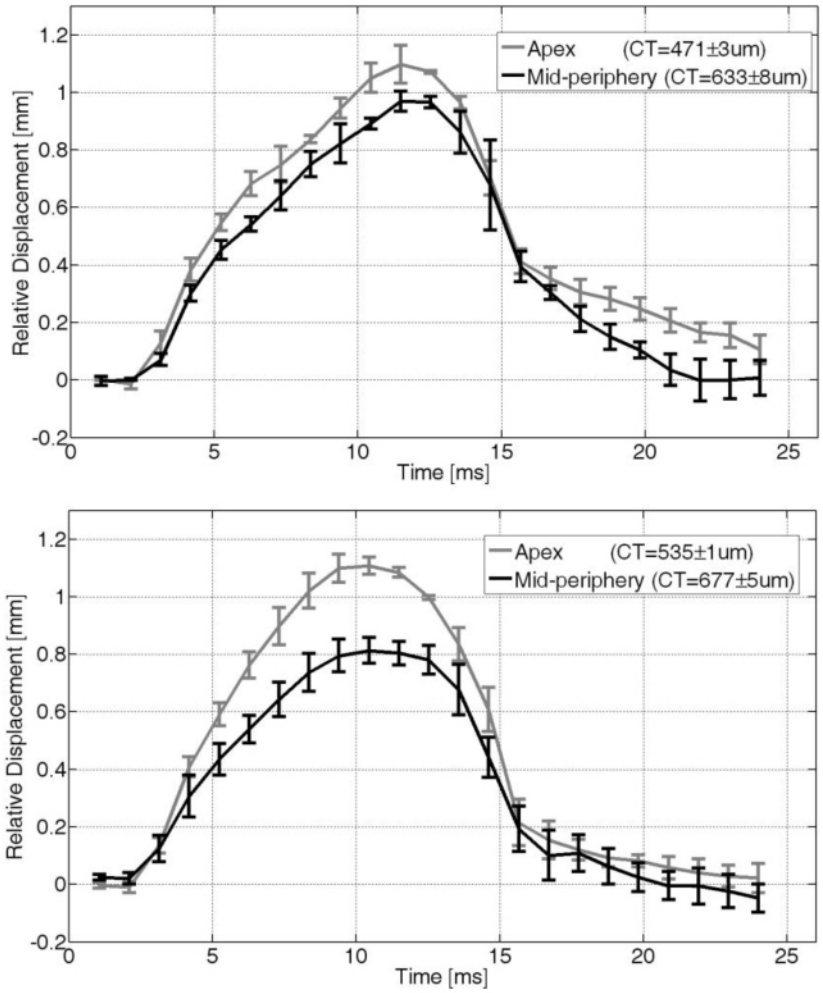

Fig. 5. Influence of the corneal location on the dynamics of the anterior corneal surface for two subjects. Error bars are ±1 SD of the mean.

3.1 Corneal localization influence on corneal dynamics

To observe the influence of corneal location and biomechanics on the dynamic behavior of the recording, two sets of measurements were taken at different corneal locations on the subject's right eye. For the first set, the subject was instructed to look through the air puff pipe and to fixate with the measured eye on the fixation light incorporated in the system. This way, it is ensured that the measurement was taken in the center of the cornea, collinearly with the axis of vision of the eye. On the second set of measurements, the subject was asked to keep the head still and look in the left direction by about 25 degrees. To help fixate with the fellow eye a cross was situated 3 meters from the subject and the subject was instructed to look at the center of the cross. Thus, the measurement was taken within the mid-periphery of the cornea. Three set of measurements were taken for each condition for two different subjects (29 and 30 year old). Figure 5 presents the averaged dynamic behavior of the cornea for the two subjects. It is worth noticing the increment on the corneal thickness (mean ± standard deviation) provided in the legend of the figure as well as the different behavior of the anterior corneal surface. With-in a subject the amplitude of the corneal displacement is more pronounced when the measurement is taken on the thinner central region of the cornea, while

#146816 - $15.00 USD Received 29 Apr 2011; revised 26 Jun 2011; accepted 27 Jun 2011; published 11 Jul 2011

the thicker peripheral region appears to allow for a lower displacement. In addition to the influence of corneal thickness, the biomechanical properties of different corneal regions may also play an important role on the obtained measurement, as the cornea has been reported to have different elastic regional properties [31]. Apart from the significant influence of the corneal thickness and biomechanics into the recordings, Fig. 5 also provides an idea on the repeatability of the measurements with respect to the alignment of the instrument. Each measurement was obtained for entirely new re-alignment of the subject. A low standard deviation value of the corneal thickness, which is provided in the legend, was obtained. This ensures that the measurement was taken at the same spot.

3.2 IOP influence on corneal dynamics

To investigate the potential influence of the IOP changes on the recorded measurement an experiment was carried out with five healthy subjects (Table 1 provides age values). After a clinical examination by an experience clinician to ensure normal ocular health, all subject had IOP measurements taken with an indentation type tonometer (Tono-Pen; Reichert Inc., Buffalo, NY). A set of three measurements was taken with the proposed technique on the central part of the cornea. After the measurements all the subjects were given a drop of Alphagan (Brimonidine tartrate 0.2%, Allergan), which reduces the production of aqueous humor and decreases pressure inside the eye, in an eye randomly selected. After one hour waiting period to ensure the drug effectiveness, a second set of three measurements was taken. Prior to the OCT tonometry, measurements of the intraocular pressure by the indentation tonometer were also completed. Table 1 shows the values of the IOP before and 1 hour after the drug was instilled into the eye. For all of the subjects a decrease in the IOP was observed, however the magnitude of pressure change varied between subjects. Table 1 also provides the corneal thickness at the point of measurement. For all of the subjects, no significantly different pachymetry values ($p<0.05$, two sample t-test) were observed between measurements. Thus, indicating that the variation on corneal displacement is not linked to the measurement variability (i.e. eye movement or instrument alignment) rather to the change in the intraocular pressure. Figure 6 presents the averaged displacement of the corneal dynamics for each of the subjects. In all of the cases, the reduction of the IOP (after drug instillation) seems to produce higher displacement of the corneal anterior surface than in baseline conditions.

Table 1. Intraocular pressure (IOP) recorded by the indentation tonometer and corneal thickness based on OCT recordings, before and 1 hour after the instillation of the drug.

Subject ID (Age)	IOP (mmHg) Baseline	IOP (mmHg) 1 hour after instillation	Corneal Thickness (μm) Baseline	Corneal Thickness (μm) 1 hour after instillation
a (29)	12	8	497±10	505±6
b (30)	13	7	505±5	511±15
c (31)	17	10	548±5	553±11
d (31)	17	8	545±14	555±9
e (37)	11	10	540±8	541±9

#146816 - $15.00 USD Received 29 Apr 2011; revised 26 Jun 2011; accepted 27 Jun 2011; published 11 Jul 2011

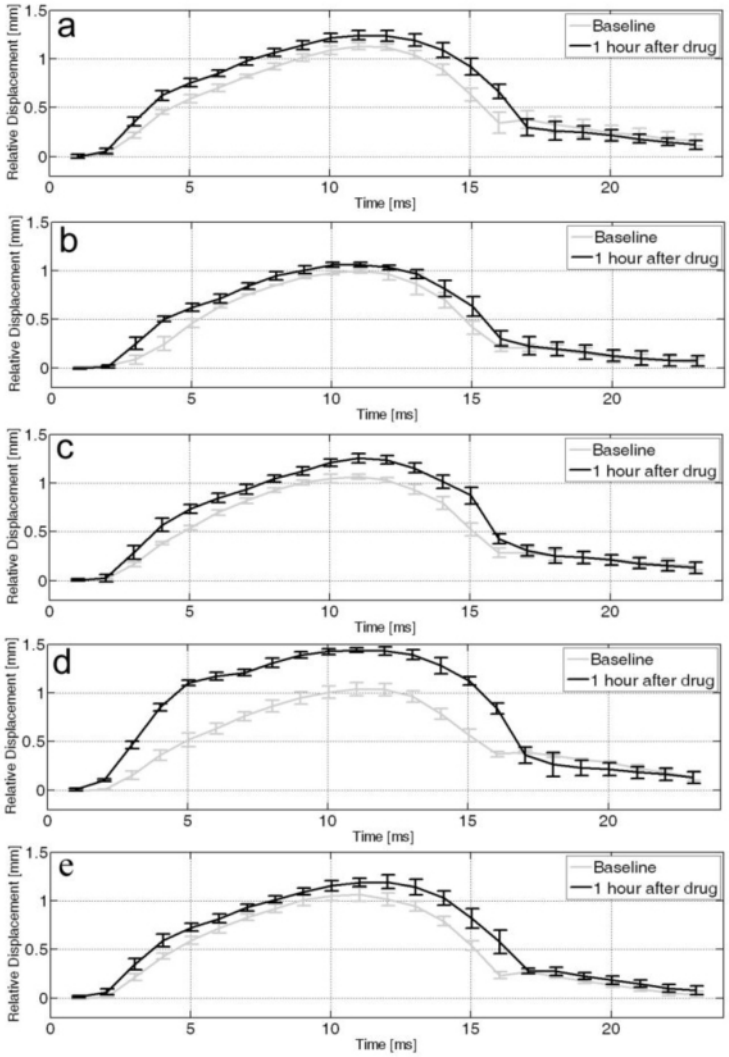

Fig. 6. Influence of the IOP reduction on the dynamics of the anterior corneal layer for 5 different subjects. Error bars are ±1 SD of the mean.

4. Discussion

In this study we have presented a swept source OCT combined with an air puff system from a non-contact tonometer. Broadly speaking, the dynamics of the anterior segment is related to the applied force (air puff), the eye intraocular pressure (IOP) and the corneal biomechanics in the eye. Thus, by having a well controlled applied force the intraocular pressure could be estimated, as well as some corneal characteristics.

To validate the setup two experiments have been performed. The first experiment looks into the effect of the corneal location on the dynamics. Based on the obtained results, with-in a subject for a constant IOP, the amplitude of the corneal displacement is more pronounced for the thinner part of the cornea (central) than for the thicker part (mid-periphery). The second experiment was performed to observe the effect of the IOP on the dynamics of the air puff stimulated cornea. The reduction of the IOP (after drug instillation) was linked with a higher displacement amplitude of the anterior corneal surface. In a recent study presented by Roberts and colleagues [14] similar behavior was observed while looking at the deformation

#146816 - $15.00 USD Received 29 Apr 2011; revised 26 Jun 2011; accepted 27 Jun 2011; published 11 Jul 2011

of the anterior segment with the high-speed Scheimpflug during the air pulse. In normal subjects, the amplitude of the layer deformation seems to be a good predictor of the IOP. While looking at the biomechanical parameters, the authors observed that for normal subjects the second strongest prediction of IOP was the corneal thickness, highlighting the influence of biomechanics on IOP [14].

A number of publications [4, 6–9, 32–34] have reported the factors that are linked to dynamic changes in the cornea during tonometry measurements (IOP measurement). The three major factors are the corneal thickness, the radius of curvature of the cornea and the viscoelastic material properties of the eye.

The effect of corneal thickness on IOP with applanation tonometric measurements has been demonstrated previously [4, 6]. From the mechanical point of view, with the same amount of pressure applied to the eye, a larger deformation will be generated for thinner corneas. Experimentally, a similar effect was observed in our study while looking at measurements at different corneal locations, despite the biomechanics can also have a secondary effect (influence) into the process. Clinically, an overestimation of the IOP has been reported for thicker corneas [8], while thinner corneas seem to produce an underestimation of the IOP [7]. This indicates that corneal thickness should be measured and compensated to get the "true IOP", which is a recommended clinical practice [2].

The radius of curvature of the cornea is also a factor likely to influence the IOP reading. This is particularly the case in applanation tonometry, which varies the applied force in order to achieve a constant area of applanation. Thus, to achieve the same area on a steeper cornea (smaller eye) it is required to apply higher force than for a flat cornea [9]. The implications of the corneal curvature for our instrument are yet to be studied. With the current system the radius may be extracted from the cross-sectional scans during the alignment period.

The corneal biomechanical properties also influence the dynamics during the air pulse. The Young's modulus (or modulus of the elasticity), which is defined as the ratio of the stress (load per unit of area) and the strain (displacement per unit area) and the Poisson's ratio, which is the material property that characterizes the deformation perpendicular to the direction of the load, are two commonly used descriptors of corneal biomechanical properties. A number of publications have reported on the link between these factors and IOP. Liu and He investigated the relation between corneal stiffness (elasticity) and IOP, a significantly higher IOP was observed for stiffened corneas when all other geometric and material properties of the eye remained constant [32]. The corneal stiffness was measured in ex vivo porcine eye by tensile testing on corneal strips [32]. In a different study the same authors introduced ultrasonic spectroscopy methods for the characterization of the corneal biomechanics [11]. A short ultrasonic pulse together with a mathematical model based on wave propagation was used to relate the reflection spectrum with cornea properties, in particular the Aggregate modulus of the cornea. This modulus is the sum of the *Lame's constant* (similar to Young modulus) and the *second Lame's constant* (the shear modulus). Another method to measure corneal elasticity was presented in [12], by means of an ultrasound microscope that measures and images the strain throughout the cornea. The technique allows the observation of the elasticity of the different corneal layers. Recently, Ford and colleagues [10] have presented an optical coherence elastography method to characterize the cornea material biomechanics. The instrument continuously images the cornea while a gonioscopy lens was used to displace the cornea by a known amount. Recordings of lateral and vertical displacement were extracted, and estimates of the shear resistance calculated.

From the clinical point of view, all of these reported factors could potentially influence IOP measurements and should be taken into account while determining the true IOP. In recent years, the accurate determination of IOP independent of corneal characteristics has been of particular interest for patients after corneal refractive surgery, as this procedure is thought to lead to errors in the accurate estimation of IOP with many current tonometry techniques, due

#146816 - $15.00 USD Received 29 Apr 2011; revised 26 Jun 2011; accepted 27 Jun 2011; published 11 Jul 2011

to changes in the cornea's structural and biomechanical properties (i.e. thickness, curvature and structure) associated with the surgery [33, 34].

In some cases, the corneal structural and biomechanical changes associated with laser refractive surgery, can also lead to the occurrence of the rare but visually debilitating condition of progressive corneal ectasia [35]. With further research and development, the proposed system in the future may also potentially be useful clinically in the screening of patients prior to refractive surgery to assist in the detection of biomechanically compromised corneas such as Forme Fruste keratoconus, as these conditions are thought to increase the risk of development of post-refractive surgery corneal ectasia [36].

Due to the fast dynamics of the corneal during acquisition, a faster laser is required to produce 2D scan (B-scans) in time. The current technique is hindered by the speed of the laser. Currently, the new FDML technology, similar to the one used in the setup, is underdevelopment and A-scans rate of up to 5Mhz have been reported [27–29]. These faster acquisition systems could allow for the wide anterior chamber characterization and corneal radius. In order to fully comprehend the system a large clinical study is required, the study could also help to determine the potential of this new instrument to enhance or produce tonometer measurements. Despite the limitations we believe that the technique proposed here is a step forward from conventional non-contact tonometer, the possibility of monitoring *in vivo* the complex anterior segment and obtain its parameter during the measurement could be a useful for the understanding and correction of IOP recordings.

5. Conclusions

Accurate IOP is a fundamental clinical indicator of the eye's health and important for the diagnosis of certain pathologies. A number of instruments are currently available to estimate the IOP, unfortunately the complexity of the measurement makes many of the current tonometers sensitivity to certain biomechanical parameters. Thus, providing IOP values that do not necessarily reflect the "true IOP" in all cases.

In this study we demonstrated a high-speed swept source optical coherence tomography combined with an air puff system. The novel instrument allows *in vivo* investigation of the corneal dynamics and the intraocular pressure during non-contact measurement by high speed acquisition of anterior segment displacement during the corneal flatting/relaxation process.

Acknowledgements

This work was supported by EuroHORCs-European Science Foundation EURYI Award EURYI-01/2008-PL (M. Wojtkowski) and Polish Ministry of Science and Higher Education Grant N N402 084435 (B. J. Kaluzny). K. Karnowski acknowledges support form Polish Ministry of Science and Higher Education Supervisor Grant N N402 482039.

#146816 - $15.00 USD Received 29 Apr 2011; revised 26 Jun 2011; accepted 27 Jun 2011; published 11 Jul 2011